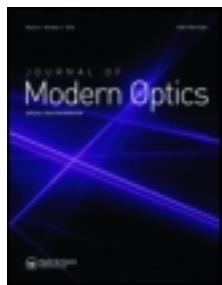


This article was downloaded by: [University of Milan], [Tom Bienaimé]

On: 27 October 2011, At: 02:31

Publisher: Taylor & Francis

Informa Ltd Registered in England and Wales Registered Number: 1072954 Registered office: Mortimer House, 37-41 Mortimer Street, London W1T 3JH, UK



Journal of Modern Optics

Publication details, including instructions for authors and subscription information:

<http://www.tandfonline.com/loi/tmop20>

Atom and photon measurement in cooperative scattering by cold atoms

T. Bienaimé^a, M. Petruzzo^b, D. Bigerni^b, N. Piovella^b & R. Kaiser^a

^a Institut Non Linéaire de Nice, CNRS, Université de Nice Sophia-Antipolis, Valbonne, 06560, France

^b Dipartimento di Fisica, Università Degli Studi di Milano, Via Celoria 16, Milano, I-20133, Italy

Available online: 12 Jul 2011

To cite this article: T. Bienaimé, M. Petruzzo, D. Bigerni, N. Piovella & R. Kaiser (2011): Atom and photon measurement in cooperative scattering by cold atoms, Journal of Modern Optics, DOI:10.1080/09500340.2011.594911

To link to this article: <http://dx.doi.org/10.1080/09500340.2011.594911>



PLEASE SCROLL DOWN FOR ARTICLE

Full terms and conditions of use: <http://www.tandfonline.com/page/terms-and-conditions>

This article may be used for research, teaching, and private study purposes. Any substantial or systematic reproduction, redistribution, reselling, loan, sub-licensing, systematic supply, or distribution in any form to anyone is expressly forbidden.

The publisher does not give any warranty express or implied or make any representation that the contents will be complete or accurate or up to date. The accuracy of any instructions, formulae, and drug doses should be independently verified with primary sources. The publisher shall not be liable for any loss, actions, claims, proceedings, demand, or costs or damages whatsoever or howsoever caused arising directly or indirectly in connection with or arising out of the use of this material.

Atom and photon measurement in cooperative scattering by cold atoms

T. Bienaimé^a, M. Petruzzo^b, D. Bigerni^b, N. Piovella^b and R. Kaiser^{a*}

^aInstitut Non Linéaire de Nice, CNRS, Université de Nice Sophia-Antipolis, Valbonne, 06560, France;

^bDipartimento di Fisica, Università Degli Studi di Milano, Via Celoria 16, Milano, I-20133, Italy

(Received 11 March 2011; final version received 24 May 2011)

In this paper, we study cooperative scattering of low intensity light by a cloud of N two-level systems. We include the incident laser field driving these two-level systems and compute the radiation pressure force on the center of mass of the cloud. This signature is of particular interest for experiments with laser cooled atoms. Including the complex coupling between dipoles in a scalar model for dilute clouds of two-level systems, we obtain expression for cooperative scattering forces taking into account the collective Lamb shift. We also derive the expression of the radiation pressure force on a large cloud of two-level systems from an heuristic approach and show that at lowest driving intensities this force is identical for a product and an entangled state.

Keywords: cold atoms; Dicke superradiance; cooperative scattering

1. Introduction

Cooperative scattering by an assembly of resonant systems has been studied in detail for many years and is based on the seminal work by R. Dicke in 1954 [1]. Related superradiance effects and collective level shifts have been studied in the context of atomic physics in the 1970s [2–4]. In the last decade, this topic has seen renewed interest [5–14] with novel experiments in nuclear physics [15] and in laser cooled clouds of atoms [16–20], applications in quantum information [21] and quantum phase transitions [22,23]. As we are mainly concerned with applications on laser cooled atomic samples, we focus in this paper on specific parameters and observables which are of interest in such experiments. We therefore derive expressions of the radiation pressure force acting on the center of mass of the atomic cloud, as well as the scattered electric field. We go beyond past approximations including the complex kernel for the coupling terms between N atoms [3,8], described by two-level systems in a scalar approach. Neglecting the complete vectorial nature of the dipole–dipole coupling seems *a priori* more justified in a dilute sample of atoms, where near field corrections are small [19]. Furthermore, we obtain the force and the radiation field as quantum operators, which may be useful for studying fluctuations and diffusion effects in radiation forces and scattered emission. Also, the imaginary part of the complex kernel, describing the collective Lamb shift, is evaluated for a gaussian density profile.

This paper is organised as follows: in Section 2, we specify the Hamiltonian used and discuss our approximations. In Section 3, we introduce the observables relevant for experiments with cold atoms, namely the radiation pressure forces on the center of mass of the atomic cloud and the scattered light intensity. The evaluation of these observables is done for specific atomic states in Section 4. We derive the result for this cooperative radiation pressure force from a more heuristic approach in Section 5. In Section 6 we discuss the relevance of the Timed Dicke State compared to a product state for this cooperative pressure force in the low intensity limit before concluding in Section 7.

2. Hamiltonian and operator equations

Our system consists of a gas of N two-level atoms (with random positions \mathbf{r}_j , lower and upper states $|g_j\rangle$ and $|e_j\rangle$ with $j=1, \dots, N$, transition frequency ω_a with linewidth $\Gamma = d^2\omega_a^3/2\pi\hbar\epsilon_0c^3$, where d is the electric dipole matrix element), driven by a uniform resonant radiation beam with wave vector $\mathbf{k}_0 = k_0\hat{e}_z$, frequency $\omega_0 = \omega_a + \Delta_0$ and electric field E_0 (see Figure 1).

The atom–field interaction Hamiltonian in the rotating-wave approximation (RWA) is

$$\hat{H} = \hat{H}_0 + \hat{H}_1, \quad (1)$$

*Corresponding author. Email: robin.kaiser@inln.cnrs.fr

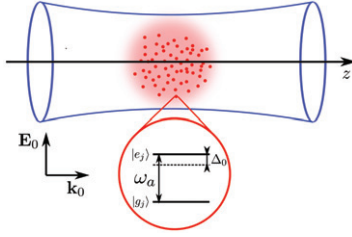


Figure 1. Experimental configuration considered: a cloud of two-level atoms is driven by an incident laser detuned by Δ_0 from the atomic resonance ω_a , with wavevector \mathbf{k}_0 . (The color version of this figure is included in the online version of the journal.)

where

$$\begin{aligned}\hat{H}_0 &= \hbar \sum_{j=1}^N \left\{ -\frac{\Delta_0}{2} \hat{\sigma}_{3j} + \frac{\Omega_0}{2} \left(\hat{\sigma}_j \exp(-i\mathbf{k}_0 \cdot \mathbf{r}_j) + \hat{\sigma}_j^\dagger \exp(i\mathbf{k}_0 \cdot \mathbf{r}_j) \right) \right\}, \\ \hat{H}_1 &= \hbar \sum_{j=1}^N \sum_{\mathbf{k}} g_{\mathbf{k}} \left[\hat{a}_{\mathbf{k}}^\dagger \hat{\sigma}_j \exp[i(\omega_{\mathbf{k}} - \omega_0)t - i\mathbf{k} \cdot \mathbf{r}_j] \right. \\ &\quad \left. + \hat{\sigma}_j^\dagger \hat{a}_{\mathbf{k}} \exp[-i(\omega_{\mathbf{k}} - \omega_0)t + i\mathbf{k} \cdot \mathbf{r}_j] \right].\end{aligned}\quad (2)$$

Here $\Omega_0 = dE_0/\hbar$ is the pump Rabi frequency, $\hat{a}_{\mathbf{k}}$ is the photon annihilation operator with wavenumber \mathbf{k} and frequency $\omega_{\mathbf{k}} = c\mathbf{k}$, $g_{\mathbf{k}} = d|\omega_{\mathbf{k}}|/(2\hbar\epsilon_0 V_{\text{ph}})^{1/2}$, V_{ph} the photon volume, $\hat{\sigma}_j = \exp(i\Delta_0 t)|g_j\rangle\langle e_j|$ and $\hat{\sigma}_{3j} = |e_j\rangle\langle e_j| - |g_j\rangle\langle g_j|$. Instead of solving the Schrödinger equation introducing some ansatz for the system state $|\Psi(t)\rangle$ [18], we write the motion equations of the atomic and field operators,

$$\begin{aligned}\frac{d\hat{\sigma}_j}{dt} &= \frac{1}{i\hbar} [\hat{\sigma}_j, \hat{H}] = i\Delta_0 \hat{\sigma}_j + \frac{i\Omega_0}{2} \hat{\sigma}_{3j} \exp(i\mathbf{k}_0 \cdot \mathbf{r}_j) \\ &\quad + i \sum_{\mathbf{k}} g_{\mathbf{k}} \hat{\sigma}_{3j} \hat{a}_{\mathbf{k}} \exp[-i(\omega_{\mathbf{k}} - \omega_0)t + i\mathbf{k} \cdot \mathbf{r}_j],\end{aligned}\quad (3)$$

$$\begin{aligned}\frac{d\hat{\sigma}_{3j}}{dt} &= \frac{1}{i\hbar} [\hat{\sigma}_{3j}, \hat{H}] = i\Omega_0 \hat{\sigma}_j \exp(-i\mathbf{k}_0 \cdot \mathbf{r}_j) \\ &\quad + 2i \sum_{\mathbf{k}} g_{\mathbf{k}} \hat{a}_{\mathbf{k}}^\dagger \hat{\sigma}_j \exp[i(\omega_{\mathbf{k}} - \omega_0)t - i\mathbf{k} \cdot \mathbf{r}_j] + \text{h.c.},\end{aligned}\quad (4)$$

$$\begin{aligned}\frac{d\hat{a}_{\mathbf{k}}}{dt} &= \frac{1}{i\hbar} [\hat{a}_{\mathbf{k}}, \hat{H}] = -ig_{\mathbf{k}} \exp[i(\omega_{\mathbf{k}} - \omega_0)t] \sum_{m=1}^N \hat{\sigma}_m \\ &\quad \times \exp(-i\mathbf{k} \cdot \mathbf{r}_m).\end{aligned}\quad (5)$$

We consider the atoms initially in their ground state and we assume weak excitation ($\Omega_0 \ll \Gamma$), so that we approximate $\hat{\sigma}_{3j}(t) \approx -\hat{I}_j$, where \hat{I}_j is the identity operator for the j th atom. This approximation amounts to neglect saturation and multi-excitation, i.e. all the processes generating more than one photon

at the same time (*linear regime*). Integrating Equation (5) and substituting it into Equation (3), neglecting $a_{\mathbf{k}}(0)$ (since the initial field state is vacuum) we obtain

$$\begin{aligned}\frac{d\hat{\sigma}_j}{dt} &= i\Delta_0 \hat{\sigma}_j - \frac{i\Omega_0}{2} \hat{I}_j \exp(i\mathbf{k}_0 \cdot \mathbf{r}_j) \\ &\quad - \sum_{\mathbf{k}} g_{\mathbf{k}}^2 \sum_{m=1}^N \exp[i\mathbf{k} \cdot (\mathbf{r}_j - \mathbf{r}_m)] \\ &\quad \times \int_0^t dt' \hat{\sigma}_m(t-t') \exp[-i(\omega_{\mathbf{k}} - \omega_0)t'].\end{aligned}\quad (6)$$

The last term in Equation (6) describes the effect of the spontaneously emitted photons on the atoms, and it is well known in the quantum electrodynamic literature [24,25]. In the Markov approximation (i.e. when the photon transit time through the atomic sample is much shorter than the excitation decay time¹), we assume under the integral $\hat{\sigma}_m(t-t') \approx \hat{\sigma}_m(t)$. The time integral then yields a real part (with a term $\delta(k - k_0)$) and an imaginary part (corresponding to the principal part of the integral). Taking into account these two terms, is at the origin of the exponential kernel, whereas the real part alone would lead to a sin kernel in Equation (9) below. We then transform the sum over the modes \mathbf{k} into an integral, $\sum_{\mathbf{k}} \rightarrow (V_{\text{ph}}/8\pi^3) \int d\mathbf{k}$. The real and imaginary parts of the double integral over t and \mathbf{k} yield the cooperative decay and frequency shift (collective Lamb shift), respectively. The proper expression of the cooperative frequency shift has been obtained adding to the Hamiltonian (2) the not-RWA contributions associated to virtual photons exchanged between different atoms. It results in the following relation [12]:

$$\begin{aligned}\sum_{\mathbf{k}} g_{\mathbf{k}}^2 \exp(i\mathbf{k} \cdot \mathbf{R}) \int_0^\infty dt' \exp[-ic(k - k_0)t'] \\ \rightarrow \frac{\Gamma}{2ik_0|\mathbf{R}|} \exp(ik_0|\mathbf{R}|),\end{aligned}\quad (7)$$

where $\Gamma = V_{\text{ph}} g_{k_0}^2 k_0^2 / (\pi c)$. Using Equation (7) in Equation (6) we obtain [12],

$$\frac{d\hat{\sigma}_j(t)}{dt} = i\Delta_0 \hat{\sigma}_j(t) - \frac{i\Omega_0}{2} \hat{I}_j \exp(i\mathbf{k}_0 \cdot \mathbf{r}_j) - \frac{\Gamma}{2} \sum_{m=1}^N \gamma_{jm} \hat{\sigma}_m(t),\quad (8)$$

where

$$\gamma_{jm} = \frac{-i \cos(k_0 r_{jm}) + \sin(k_0 r_{jm})}{k_0 r_{jm}} = \frac{\exp(ik_0 r_{jm})}{ik_0 r_{jm}}\quad (9)$$

and $r_{jm} = |\mathbf{r}_j - \mathbf{r}_m|$. Equations (8) describe the time evolution of the atomic operators for N weakly excited atoms scattering radiation. The real part of γ_{jm} describes the spontaneous emission decay and the

imaginary part of γ_{jm} describes the energy shift due to resonant dipole–dipole interactions. A slightly different approach can be used to derive this result as shown in Appendix 1. Note that even though this result will yield a density dependent collective shift of the resonance, we use a scalar model for the field, neglecting thus any polarization and near field dependence [10,13]. Detailed calculations for small and large samples of various geometries, however, show that near field and far field contributions as well as resonant and antiresonant terms need to be taken properly into account for quantitative predictions [3,13,14], and the present model thus needs to be considered with care illustrating only a part of the dipole–dipole coupling for real systems.

Equation (8) can also be cast in the form

$$\frac{d\hat{\sigma}_j}{dt} = \frac{1}{i\hbar} [\hat{\sigma}_j, \hat{H}_0 + \hat{H}_{\text{eff}}], \quad (10)$$

where

$$\begin{aligned} \hat{H}_0' &= \hbar \sum_{j=1}^N \left\{ -\Delta_0 \hat{\sigma}_j^\dagger \hat{\sigma}_j + \frac{\Omega_0}{2} \left(\hat{\sigma}_j \exp(-i\mathbf{k}_0 \cdot \mathbf{r}_j) \right. \right. \\ &\quad \left. \left. + \hat{\sigma}_j^\dagger \exp(i\mathbf{k}_0 \cdot \mathbf{r}_j) \right) \right\}, \\ \hat{H}_{\text{eff}} &= \frac{\hbar\Gamma}{2} \sum_{j,m} \frac{\exp(i\mathbf{k}_0 \cdot \mathbf{r}_{jm})}{i\mathbf{k}_0 \cdot \mathbf{r}_{jm}} \hat{\sigma}_j^\dagger \hat{\sigma}_m \end{aligned} \quad (11)$$

and the commutation rules in the *linear regime* are $[\hat{\sigma}_j, \hat{\sigma}_m^\dagger] = \delta_{jm}$.

3. Observables

Among the different observables of the system, scattered light and radiation pressure force contain important signatures of cooperative scattering. Concerning scattered radiation, the positive-frequency part of the electric field is defined as

$$\hat{E}(\mathbf{r}, t) = i \sum_{\mathbf{k}} \mathcal{E}_k \hat{a}_{\mathbf{k}}(t) \exp(-i\omega_{\mathbf{k}} t + i\mathbf{k} \cdot \mathbf{r}), \quad (12)$$

where $\mathcal{E}_k = (\hbar\omega_k/2\epsilon_0 V_{\text{ph}})^{1/2}$ is the single-photon electric field. By integrating Equation (5) and inserting it in Equation (12) we obtain

$$\begin{aligned} \hat{E}(\mathbf{r}, t) &= \sum_{\mathbf{k}} \mathcal{E}_k g_{\mathbf{k}} \sum_{m=1}^N \exp[i\mathbf{k} \cdot (\mathbf{r} - \mathbf{r}_m) - i\omega_{\mathbf{k}} t] \int_0^t dt' \\ &\quad \times \exp[-i(\omega_{\mathbf{k}} - \omega_0)t'] \hat{\sigma}_m(t-t'). \end{aligned} \quad (13)$$

Using Equation (7), the Markov approximation leads to

$$\hat{E}(\mathbf{r}, t) \approx -i \frac{dk_0^2}{4\pi\epsilon_0} \sum_{j=1}^N \frac{\exp[-i\omega_0(t - |\mathbf{r} - \mathbf{r}_j|/c)]}{|\mathbf{r} - \mathbf{r}_j|} \hat{\sigma}_j(t), \quad (14)$$

which has a transparent interpretation as the sum of wavelets scattered by N dipoles of position \mathbf{r}_j and detected at distance \mathbf{r} and time t . In the far field limit, $|\mathbf{r} - \mathbf{r}_j| \approx r - (\mathbf{r} \cdot \mathbf{r}_j)/r$ and

$$\hat{E}(\mathbf{r}, t) \approx -i \frac{dk_0^2}{4\pi\epsilon_0 r} \exp[-i\omega_0(t - r/c)] \sum_{j=1}^N \exp(-i\mathbf{k}_s \cdot \mathbf{r}_j) \hat{\sigma}_j(t), \quad (15)$$

where $\mathbf{k}_s = k_0(\mathbf{r}/r)$.

The radiation pressure force acting on the j th atom has been calculated from Equation (1) as $\hat{\mathbf{F}}_j = -\nabla_{\mathbf{r}_j} \hat{H} = \hat{\mathbf{F}}_{aj} + \hat{\mathbf{F}}_{ej}$, where [18]

$$\hat{\mathbf{F}}_{aj} = i\hbar k_0 \frac{\Omega_0}{2} \left\{ \exp(-i\mathbf{k}_0 \cdot \mathbf{r}_j) \hat{\sigma}_j - \text{h.c.} \right\}, \quad (16)$$

$$\begin{aligned} \hat{\mathbf{F}}_{ej} &= i\hbar \sum_{\mathbf{k}} \mathbf{k} g_{\mathbf{k}} \left\{ \hat{a}_{\mathbf{k}}^\dagger \hat{\sigma}_j \exp[i(\omega_{\mathbf{k}} - \omega_0)t - i\mathbf{k} \cdot \mathbf{r}_j] \right. \\ &\quad \left. - \hat{\sigma}_j^\dagger \hat{a}_{\mathbf{k}} \exp[-i(\omega_{\mathbf{k}} - \omega_0)t + i\mathbf{k} \cdot \mathbf{r}_j] \right\}, \end{aligned} \quad (17)$$

where $\hat{\mathbf{F}}_{aj}$ and $\hat{\mathbf{F}}_{ej}$ result from the recoil received upon absorption of a photon from the pump and from the emission of a photon into any direction \mathbf{k} , respectively. Eliminating the field using Equation (5), Equation (17) becomes

$$\begin{aligned} \hat{\mathbf{F}}_{ej}(t) &= -\hbar \sum_{\mathbf{k}} \mathbf{k} g_{\mathbf{k}}^2 \left\{ \sum_{m=1}^N \exp[-i\mathbf{k} \cdot (\mathbf{r}_j - \mathbf{r}_m)] \int_0^t dt' \right. \\ &\quad \times \exp[i(\omega_{\mathbf{k}} - \omega_0)t'] \hat{\sigma}_m^\dagger(t-t') \hat{\sigma}_j(t) \\ &\quad + \hat{\sigma}_j^\dagger(t) \sum_{m=1}^N \exp[i\mathbf{k} \cdot (\mathbf{r}_j - \mathbf{r}_m)] \int_0^t dt' \\ &\quad \left. \times \exp[-i(\omega_{\mathbf{k}} - \omega_0)t'] \hat{\sigma}_m(t-t') \right\}. \end{aligned} \quad (18)$$

Assuming the Markov approximation, $\hat{\sigma}_m(t-t') \approx \hat{\sigma}_m(t)$, then Equation (18) becomes

$$\begin{aligned} \hat{\mathbf{F}}_{ej}(t) &= -\hbar \sum_{m=1}^N \sum_{\mathbf{k}} \mathbf{k} g_{\mathbf{k}}^2 \left\{ \hat{\sigma}_m^\dagger(t) \hat{\sigma}_j(t) \exp(-i\mathbf{k} \cdot \mathbf{r}_{jm}) \int_0^t dt' \right. \\ &\quad \times \exp[i(\omega_{\mathbf{k}} - \omega_0)t'] \\ &\quad \left. + \hat{\sigma}_j^\dagger(t) \hat{\sigma}_m(t) \exp(i\mathbf{k} \cdot \mathbf{r}_{jm}) \int_0^t dt' \exp[-i(\omega_{\mathbf{k}} - \omega_0)t'] \right\}, \end{aligned} \quad (19)$$

where $\mathbf{r}_{jm} = \mathbf{r}_j - \mathbf{r}_m$. The force (19) acting on the j th atom has a single-atom contribution $\hat{\mathbf{F}}_{ej}^{(\text{self})}$ (term $m=j$ in the sum) accounting for its own photon emission recoil, and a contribution $\hat{\mathbf{F}}_{ej}^{(\text{int})}$ (terms $m \neq j$) accounting for coupling between the j th atom and all the other atoms. Note that this dipole–dipole interaction can occur via a coupling to common vacuum modes of

radiation. The interference terms in the total scattered field can leave a fingerprint on the forces acting on the atoms inside the cloud. The first contribution yields

$$\hat{\mathbf{F}}_{ej}^{(\text{self})} \approx -\hbar\Gamma \sum_{|\mathbf{k}|=k_0} \mathbf{k} \hat{\sigma}_j^\dagger \hat{\sigma}_j, \quad (20)$$

where the sum is over all the randomly oriented modes $\mathbf{k} = k_0 \hat{\mathbf{k}}$ and we have omitted the self-energy shift (Lamb shift) coming from the principal part term of the time integral in Equation (19). Noting that for $m \neq j$ we have $i\mathbf{k} \exp(i\mathbf{k} \cdot \mathbf{r}_{jm}) = \nabla_{\mathbf{r}_j} \exp(i\mathbf{k} \cdot \mathbf{r}_{jm})$, the second contribution to Equation (19) can be written as

$$\begin{aligned} \hat{\mathbf{F}}_{ej}^{(\text{int})}(t) &= -i\hbar \nabla_{\mathbf{r}_j} \sum_{m \neq j} \sum_{\mathbf{k}} g_k^2 \left\{ \hat{\sigma}_j(t) \hat{\sigma}_m^\dagger(t) \exp(-i\mathbf{k} \cdot \mathbf{r}_{jm}) \right. \\ &\quad \times \left. \int_0^t dt' \exp[i(\omega_k - \omega_0)t'] - \text{h.c.} \right\}. \end{aligned} \quad (21)$$

Using Equation (7) in Equation (21), Equation (19) becomes

$$\hat{\mathbf{F}}_{ej}(t) = \hat{\mathbf{F}}_{ej}^{(\text{self})}(t) - \nabla_{\mathbf{r}_j} \sum_{m \neq j} \hat{V}_{jm}(t), \quad (22)$$

where

$$\begin{aligned} \hat{V}_{jm}(t) &= -\frac{\hbar\Gamma}{2} \\ &\quad \times \left\{ \frac{\hat{\sigma}_j^\dagger(t) \hat{\sigma}_m(t) \exp(-ik_0 r_{jm}) + \hat{\sigma}_j(t) \hat{\sigma}_m^\dagger(t) \exp(ik_0 r_{jm})}{k_0 r_{jm}} \right\} \end{aligned} \quad (23)$$

is the effective interaction energy between j th and m th atoms. Since $\nabla_{\mathbf{r}_j} [\exp(ik_0 r)/r] = \mathbf{r}(ik_0 r - 1) \exp(ik_0 r)/r^3$, Equation (22) becomes

$$\begin{aligned} \hat{\mathbf{F}}_{ej} &= \hat{\mathbf{F}}_{ej}^{(\text{self})} - \frac{\hbar k_0 \Gamma}{2} \sum_{m=1}^N \frac{\hat{\mathbf{n}}_{jm}}{(k_0 r_{jm})^2} \\ &\quad \times \left\{ \hat{\sigma}_j^\dagger \hat{\sigma}_m (1 + ik_0 r_{jm}) \exp(-ik_0 r_{jm}) + \text{h.c.} \right\}, \end{aligned} \quad (24)$$

where $\hat{\mathbf{n}}_{jm} = \mathbf{r}_{jm}/r_{jm}$. The emission force acting on the j th atom has two contributions: (a) a self-force due to its own photon emission; (b) a force due to the dipole-dipole interactions with all the other atoms. This second force has a term decreasing as $1/r_{jm}$ and one decreasing as $1/r_{jm}^2$.

4. Atomic state

The linear approximation assumed in the equations of the atomic operators $\hat{\sigma}_j$, Equation (8), suggests that we may restrict the Hilbert space of the N atoms to the

subspace spanned by the ground state $|g\rangle = |g_1, \dots, g_N\rangle$ and the single-excited-atom states $|j\rangle = |g_1, \dots, e_j, \dots, g_N\rangle$ with $j=1, \dots, N$. Hence, we set

$$|\Psi(t)\rangle = \alpha(t)|g\rangle + \exp(-i\Delta_0 t) \sum_{j=1}^N \beta_j(t)|j\rangle, \quad (25)$$

where we will approximate $\alpha \approx 1$ after having evaluated the different expectation values, e.g. $\langle \hat{\sigma}_j \rangle \approx \beta_j$ and $\langle \hat{\sigma}_j^\dagger \hat{\sigma}_m \rangle \approx \beta_j^* \beta_m$. So, Equation (8) yields

$$\begin{aligned} \frac{d\beta_j(t)}{dt} &= \left(i\Delta_0 - \frac{\Gamma}{2} \right) \beta_j(t) - \frac{i\Omega_0}{2} \exp(i\mathbf{k}_0 \cdot \mathbf{r}_j) \\ &\quad - \frac{\Gamma}{2} \sum_{j \neq m} \gamma_{jm} \beta_m(t), \end{aligned} \quad (26)$$

with initial conditions $\beta_j(0)=0$. The self-interaction term, $\Gamma \gamma_{jj} = \Gamma - i\Delta \Omega_{\text{LS}}$ yields the single-atom spontaneous decay Γ and the single-atom Lamb shift $\Delta \Omega_{\text{LS}}$, which can be reabsorbed in the definition of the atomic frequency ω_a , and will be neglected in the present analysis.

Considering the force applied to the center of mass of the atomic ensemble, $\hat{\mathbf{F}} = (1/N) \sum_j \hat{\mathbf{F}}_j$, from Equations (16) and (24) the components along the z axis are

$$\langle \hat{F}_{az} \rangle = \hbar k_0 \frac{\Omega_0}{N} \sum_{j=1}^N \text{Im} \left(\exp(i\mathbf{k}_0 \cdot \mathbf{r}_j) \beta_j \right), \quad (27)$$

$$\langle \hat{F}_{ez} \rangle = -\frac{\hbar k_0 \Gamma}{2N} \sum_{j \neq m} \hat{z}_{jm} j_1(k_0 r_{jm}) i(\beta_j^* \beta_m - \text{c.c.}), \quad (28)$$

where $j_1(z) = \sin(z)/z^2 - \cos(z)/z$ is the first-order spherical Bessel function and $\hat{z}_{jm} = (z_j - z_m)/r_{jm}$. Note also that the self-force (20) has zero average since $\sum_{\mathbf{k}} \mathbf{k} = 0$ (although in general its fluctuations are different from zero).

Also, from Equation (15) it is possible to obtain the average intensity of the scattered radiation as a function of the atomic wave function,

$$\begin{aligned} I(\mathbf{r}, t) &= \epsilon_0 c \langle \hat{E}^\dagger(\mathbf{r}, t) \hat{E}(\mathbf{r}, t) \rangle \\ &= \left(\frac{d^2 \omega_0^4}{16\pi^2 \epsilon_0 c^3 r^2} \right) \left| \sum_{j=1}^N \exp(-i\mathbf{k}_s \cdot \mathbf{r}_j) \beta_j(t) \right|^2. \end{aligned} \quad (29)$$

The state (25) may be conveniently expressed in the timed Dicke (TD) basis, introduced originally by Dicke [1] and successively considered by Friedberg and coworkers [3] for their study on cooperative Lamb shift and by Scully and coworkers [6,9] to describe cooperative decay of N atoms prepared in a symmetric phased state. The completely symmetric TD state is

$|+\rangle_{k_0} = (1/N^{1/2}) \sum_j \exp(i\mathbf{k}_0 \cdot \mathbf{r}_j) |j\rangle$ and Equation (25) can be written as

$$|\Psi(t)\rangle = \alpha(t)|g\rangle + \exp(-i\Delta_0 t) \beta_{\text{TD}}(t) |+\rangle_{k_0} + \exp(-i\Delta_0 t) \sum_{s=1}^{N-1} \gamma_s(t) |s\rangle_{k_0}, \quad (30)$$

where $|s\rangle_{k_0}$ groups all the states orthogonal to $|+\rangle_{k_0}$ [6].

A numerical analysis of Equation (26) shows that, for a constant driving field Ω_0 and for atomic cloud sizes much larger than the optical wavelength, the occupation probability of the states $|s\rangle_{k_0}$ is only a small fraction of the atomic state [20] and it is in general negligible, so that Equation (26) becomes

$$\frac{d\beta_{\text{TD}}}{dt} = -\frac{i}{2} N^{1/2} \Omega_0 + i(\Delta_0 - \Delta_N) \beta_{\text{TD}} - \frac{1}{2} \Gamma N s_N \beta_{\text{TD}}, \quad (31)$$

where

$$s_N = \frac{1}{N^2} \sum_{j,m=1}^N \frac{\sin(k_0 |\mathbf{r}_j - \mathbf{r}_m|)}{k_0 |\mathbf{r}_j - \mathbf{r}_m|} \exp[-i\mathbf{k}_0 \cdot (\mathbf{r}_j - \mathbf{r}_m)] = \frac{1}{4\pi} \int_0^{2\pi} d\phi \int_0^\pi d\theta \sin\theta |S_N(k_0, \theta, \phi)|^2, \quad (32)$$

$$\Delta_N = -\frac{\Gamma}{2N} \sum_{j \neq m}^N \frac{\cos(k_0 |\mathbf{r}_j - \mathbf{r}_m|)}{k_0 |\mathbf{r}_j - \mathbf{r}_m|} \exp[-i\mathbf{k}_0 \cdot (\mathbf{r}_j - \mathbf{r}_m)] = -\frac{\Gamma N}{8\pi^2} \text{P} \int_0^\infty \frac{d\kappa \kappa^3}{\kappa - 1} \int_0^{2\pi} d\phi \int_0^\pi d\theta \sin\theta |S_N(k_0 \kappa, \theta, \phi)|^2, \quad (33)$$

where $\kappa = k/k_0$,

$$S_N(\mathbf{k}) \equiv \frac{1}{N} \sum_{j=1}^N \exp[-i(\mathbf{k} - \mathbf{k}_0) \cdot \mathbf{r}_j] \quad (34)$$

is the factor form and the integral over κ in Equation (33) is evaluated as a principal part. The term Δ_N is the collective Lamb frequency shift [3,10]. At steady state we find

$$\beta_{\text{TD}} = \frac{\Omega_0 N^{1/2}}{2(\Delta_0 - \Delta_N) + iN\Gamma s_N}, \quad (35)$$

and

$$\langle \hat{F}_z \rangle = \langle \hat{F}_{az} \rangle + \langle \hat{F}_{ez} \rangle = \hbar k_0 \Gamma \frac{\Omega_0^2}{4(\Delta_0 - \Delta_N)^2 + N^2 \Gamma^2 s_N^2} N[s_N - f_N], \quad (36)$$

where

$$f_N = \frac{1}{N^2} \sum_{j \neq m} \hat{z}_{jm} j_1(k_0 r_{jm}) \sin(k_0 z_{jm}). \quad (37)$$

The cooperative radiation force can be obtained from the standard single-atom radiation pressure force $F_1 = \hbar k_0 \Gamma \Omega_0^2 / (4\Delta_0^2 + \Gamma^2)$ substituting the natural linewidth by the collective linewidth, $\Gamma_N = \Gamma N s_N$, and multiplying it by $1 - f_N/s_N$, where f_N/s_N is the probability to observe the photon emitted in the forward direction. Isolating the term $j = m$,

$$|S_N(\mathbf{k})|^2 = \frac{1}{N} + \sum_{j \neq m} \exp[i(\mathbf{k}_0 - \mathbf{k}) \cdot (\mathbf{r}_j - \mathbf{r}_m)] \approx \frac{1}{N} + |S_\infty(\mathbf{k})|^2, \quad (38)$$

where the factor form $S_\infty(\mathbf{k})$ is evaluated for a continuous approximation with density distribution $n(\mathbf{r})$,

$$S_\infty(\mathbf{k}) = \frac{1}{N} \int_V d\mathbf{r} n(\mathbf{r}) \exp[i(\mathbf{k}_0 - \mathbf{k}) \cdot \mathbf{r}]. \quad (39)$$

Then, $s_N \approx (1/N) + s_\infty$ and $f_N \approx f_\infty$ where,

$$s_\infty = \frac{1}{4\pi} \int d\Omega_k |S_\infty(\mathbf{k})|^2, \quad f_\infty = \frac{1}{4\pi} \int d\Omega_k \cos\theta |S_\infty(\mathbf{k})|^2 \quad (40)$$

and Equation (36) becomes

$$F_z = \frac{\hbar k_0 \Gamma \Omega_0^2}{4(\Delta - \Delta_N)^2 + \Gamma_N^2} \left[1 + \frac{N}{4\pi} \int d\Omega_k (1 - \cos\theta) |S_\infty(\mathbf{k})|^2 \right]. \quad (41)$$

The factor form $S_\infty(\mathbf{k})$ and the integrated factors s_∞ and f_∞ have been calculated in [18] for a Gaussian density distribution with ellipsoidal profile, $n(\mathbf{r})_0 \exp[-(x^2 + y^2)/2\sigma_r^2 - z^2/2\sigma_z^2]$, yielding $S_\infty(k_0, \theta) = \exp\{-\sigma^2[\sin^2\theta + \eta^2(\cos\theta - 1)^2]/2\}$, where $\sigma = k_0 \sigma_r$ and $\eta = \sigma_z/\sigma_r$ is the aspect ratio. For spherical and large clouds ($\eta = 1$ and $\sigma \gg 1$), $s_\infty \approx 1/(4\sigma^2)$, $f_\infty \approx s_\infty - 1/(8\sigma^4)$ and the collective Lamb shift is $\Delta_N \approx \Delta_\infty$ where (see [14] and Appendix 2)

$$\Delta_\infty = -\frac{\Gamma N}{4\pi^{1/2} \sigma^3}, \quad (42)$$

which is a redshift, proportional to the number of atoms in a cubic wavelength [3], i.e. atomic density and not optical thickness $b_0 = 3N/\sigma^2$. These values for s_∞ , f_∞ and Δ_∞ can be compared to numerical evaluation of the s_N , f_N and Δ_N for a finite number of atoms and a specific configuration. In Figure 2 we show the distribution of these values for different sample size.

In our numerical simulations shown in Figure 3 we observe strong configuration dependent fluctuations for the value of the collective Lamb shift. A precise comparison with our analytical expression, valid for large clouds, is thus cumbersome and did not allow us to validate precise predictions of the numerical factor in Equation (42).

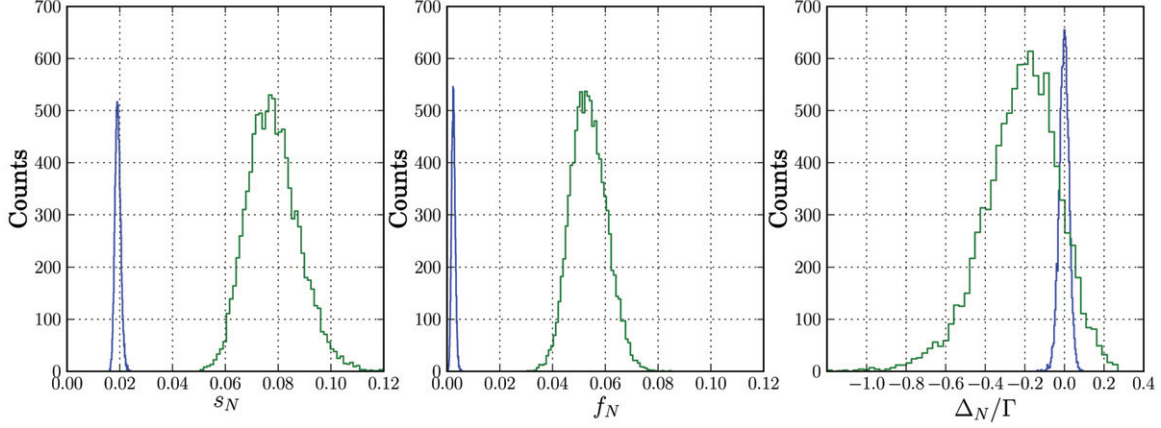


Figure 2. Distributions for values of s_N , f_N and Δ_N for $N=50$ atoms, plotted for 10,000 configurations for a size corresponding to $\sigma=10$ (blue curves) and $\sigma=2$ (green curves). (The color version of this figure is included in the online version of the journal.)

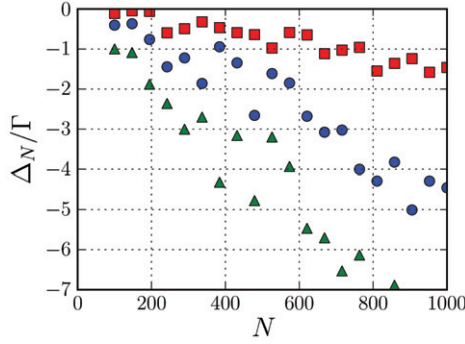


Figure 3. Collective Lamb shift versus atom number for $\sigma=1.6$ (green triangles) $\sigma=2$ (blue circles) and $\sigma=3$ (red squares). (The color version of this figure is included in the online version of the journal.)

Normalizing the radiation pressure force with respect to the single atom value, we obtain for large atomic samples,

$$\frac{\langle \hat{F}_z \rangle}{F_1} = \frac{4\Delta_0^2 + \Gamma^2}{4(\Delta_0 - \Delta_N)^2 + \Gamma^2(1 + b_0/12)^2} \left[1 + \frac{b_0}{24\sigma^2} \right]. \quad (43)$$

Finally, from Equation (29) we obtain the scattered intensity

$$I(\mathbf{r}) = \left(\frac{I_0}{16\pi^2 k_0^2 r^2} \right) \left[\frac{\Gamma^2}{4(\Delta_0 - \Delta_N)^2 + \Gamma^2(1 + b_0/12)^2} \right] \times [N + N^2 |S_\infty(\mathbf{k}_s)|^2]. \quad (44)$$

This expression of the scattered intensity illustrates the role of the shape of the atomic cloud for the modified emission diagram. The emission diagram of the TD state is shown in Figure 4. It illustrates the strong

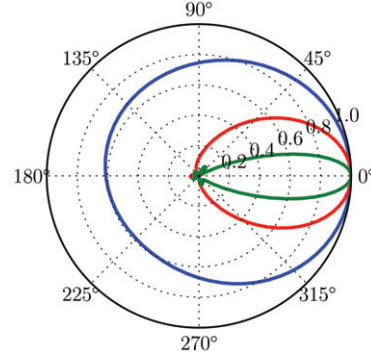


Figure 4. Emission diagram computed according to Equation (29) for the Tamed Dicke state $|+\rangle_{k_0}$ with $N=40$ atoms: $\sigma=0.4$ (blue), $\sigma=1$ (red), $\sigma=8$ (green). (The color version of this figure is included in the online version of the journal.)

forward emission by the cloud when its size exceeds a few optical wavelengths, reminiscent of Mie scattering, or more precisely of Rayleigh–Debye–Gans [26]. As we will discuss in the following section, a modified emission diagram yields a modified radiation pressure force, as the recoil of the scattered photon (partially) compensates the recoil effect at absorption.

5. Heuristic approach

The result (36) can be interpreted heuristically considering the momentum balance in a given time interval δt [27]. During δt , N two-level atoms with positions \mathbf{r}_j ($j=1, \dots, N$) do δN fluorescence cycles, each time absorbing a photon with momentum $\hbar\mathbf{k}_0$ from the laser and emitting a photon with momentum

$\hbar\mathbf{k}_i$ ($i=1, \dots, \delta N$) in a random direction $\boldsymbol{\Omega}_i$, with probability $P_{i,j}=P(\boldsymbol{\Omega}_i, \mathbf{r}_j)$. The momentum variation for the j th atom after δN cycles is

$$\delta p_j = (\hbar\mathbf{k}_0)\delta N - \sum_{i=1}^{\delta N} (\hbar\mathbf{k}_i)P_{i,j}. \quad (45)$$

For a single isolated atom the emission is isotropic and $P_{i,j}=1$, but for N atoms the emission may not be isotropic depending on the atomic distribution. Also, the excitation could be nonuniform if the phase front of the driving beam is getting distorted by the refractive index changes in the atomic cloud. Assuming for simplicity that the excitation is uniform over the entire atomic ensemble and neglecting phase distortion effects [28,29], δN will be the same for all the atoms and $|\mathbf{k}_i|=k_0$. Considering the momentum variation along the direction of the incident photon (z axis), after averaging over the atoms

$$\delta p_z = \frac{1}{N} \sum_{j=1}^N \delta p_{j,z} = (\hbar k_0)\delta N - (\hbar k_0) \sum_{i=1}^{\delta N} P_i \cos \theta_i, \quad (46)$$

where $P_i = (1/N) \sum_j P_{i,j} = P(\cos \theta_i)$ is the emission probability along the angle θ_i . Considering $\cos \theta_i$ and δN as independent random variables, the statistical average of Equation (46) is

$$\overline{\delta p_z} = (\hbar k_0) \overline{\delta N} - (\hbar k_0) \overline{\delta N} \cdot \overline{\cos \theta}, \quad (47)$$

where we assumed $\overline{\sum_i \cos \theta_i} \approx \overline{\delta N} \cdot \overline{\cos \theta}$. Hence, the pressure force is

$$F_z = \frac{\overline{\delta p_z}}{\delta t} = (\hbar k_0) \left(\frac{\overline{\delta N}}{\delta t} \right) [1 - \overline{\cos \theta}]. \quad (48)$$

Comparing with Equation (36) we found the following correspondence

$$\left(\frac{\overline{\delta N}}{\delta t} \right) = \frac{\Omega_0^2 \Gamma_N}{4(\Delta - \Delta_N)^2 + \Gamma_N^2}, \quad \overline{\cos \theta} = \frac{f_N}{s_N}, \quad (49)$$

where $\Gamma_N = \Gamma_N s_N$. So, the scattering rate $(\overline{\delta N}/\delta t)$ is equal to the excitation probability, $\rho_{ee} = \Omega_0^2/[4(\Delta - \Delta_N)^2 + \Gamma_N^2]$, times the collective decay rate, Γ_N . The radiation pressure force (36) is equal to the momentum photon, $\hbar k_0$, multiplied by the scattering rate and by a geometrical factor $1 - \overline{\cos \theta}$ taking into account the directionality of the scattered light. Cooperativity modifies both the scattering rate, enhancing the decay rate and shifting the resonance frequency, and the scattering direction. Small samples tend to radiate isotropically whereas extended samples radiate super-radiantly in the forward direction [11,18]. These cooperative effects can be revealed measuring radiation pressure force by monitoring center-of-mass motion of large atomic clouds released by magneto-optical traps

[16,17], and then identifying fast decay, shifts and modified emission diagrams described by Equations (36) and (44).

6. Product state

It has been noted that the same results obtained for a symmetric TD state could be obtained assuming a product state for N atoms [5,13] (named also ‘Bloch state’ by some authors [7]):

$$|\Psi(t)\rangle_c = \prod_{j=1}^N \{ \alpha_c(t) |g_j\rangle + \beta_c(t) \exp(i\mathbf{k}_0 \cdot \mathbf{r}_j - i\Delta_0 t) |e_j\rangle \}, \quad (50)$$

where $\alpha_c(t)$ and $\beta_c(t)$ are the same for every atom, with $|\alpha_c(t)|^2 + |\beta_c(t)|^2 = 1$. The ansatz of Equation (50) assumes each j th atom driven into the excited state with equal probability $|\beta_c(t)|^2$ and phase $\phi_j = \mathbf{k}_0 \cdot \mathbf{r}_j - \Delta_0 t$. As it happens for the symmetric TD state (30), the driving field imposes a coherence in the photons emitted spontaneously by each atom, so that super-radiance arises because the state is symmetric under exchange of particles [30]. However, it is expected that the quantum statistic of the symmetric TD state will be quite different from that of the ‘quasi-classical’ product state. Notice that for $|\beta_c| \ll 1$ the product state (50) can be written in the following form [7,14]

$$|\Psi\rangle_c = \alpha_c^N |g\rangle + \alpha_c^{N-1} \beta_c \sum_j \exp(i\mathbf{k}_0 \cdot \mathbf{r}_j - i\Delta_0 t) |j\rangle + \alpha_c^{N-2} \beta_c^2 \sum_{j \neq m} \exp[i\mathbf{k}_0 \cdot (\mathbf{r}_j + \mathbf{r}_m) - 2i\Delta_0 t] |j, m\rangle + \dots, \quad (51)$$

where $|j, m\rangle = |g_1, \dots, e_j, \dots, e_m, \dots, g_N\rangle$. Hence, the product state can be expanded in the *symmetric* TD states with 1 to N excited atoms. Only in the limits $\alpha_c \approx 1$ and $|\beta_c| \ll 1$ the product state reduces to the symmetric single-excited atom state $|\psi\rangle \approx |g\rangle + \beta_c N^{1/2} |+\rangle_{\mathbf{k}_0}$ if only the first two terms of Equation (51) are retained. The expectation values for the state (50) are $\langle \hat{\sigma}_j \rangle = \alpha_c^* \beta_c$ and $\langle \hat{\sigma}_m^\dagger \hat{\sigma}_j \rangle = |\alpha_c|^2 |\beta_c|^2$, so for $\alpha_c \approx 1$ they coincide with those obtained from the symmetric TD state. Differences between the product and the symmetric TD states should appear when higher-order expectation values are observed, as for instance $\langle \hat{\sigma}_j \hat{\sigma}_m \rangle$, which is zero for the TD state and $\alpha_c^{*2} \beta_j \beta_m \approx \beta_j \beta_m$ for the product state. Notice that operator ordering produces different results in high-order expectation values if scattered photons or atomic forces are measured. These features and non-classical effects studies in cooperative scattering by cold atoms will be the object of a future investigation.

7. Conclusion

In this paper, we have included a more precise kernel to evaluate the cooperative radiation pressure force on a cloud of two-level systems. The collective Lamb shift leads to a shift Δ_N of the resonance, which is proportional to the spatial density. As we have used a scalar model in this paper, near field and polarization effects are neglected. One thus needs to consider this shift with some scepticism as the numerical factor for this shift in a real system will be strongly modified by the vectorial nature of the light [3]. For dilute clouds, we recover previous results [16], where these density effects are negligible. We also presented a simple model to estimate the radiation pressure force from the modified emission diagram and assuming coupling to the single photon superradiant (Timed Dicke) state [6]. This approach can be useful to estimate not only average forces but also fluctuations and dissipation. Finally, we noted that in the low intensity limit, the average result we derived for the cooperative radiation pressure force can be obtained either by assuming a driven Timed Dicke state or a product state [5,7,13], with no entanglement required. Looking for non-classical features in cooperative scattering of light by a cloud of two-level system thus requires studies of higher orders either by using higher intensities or looking at correlations or fluctuations of the force.

Acknowledgements

We acknowledge fruitful discussions with E. Akkermans, P. Courteille, M. Havey, I. Sokolov and stimulating presentations on this topic at the PQE 2011 conference.

Note

1. Light may propagate in dense atomic samples with a group velocity smaller than c [31]. In this case the Markov approximation should be satisfied by a more stringent condition.

References

- [1] Dicke, R.H. *Phys. Rev.* **1954**, *93*, 99–110.
- [2] Lehmberg, R. *Phys. Rev. A* **1968**, *2*, 883–888.
- [3] Friedberg, R.; Hartmann, S.R.; Manassah, J.T. *Phys. Rep.* **1973**, *7*, 101–179.
- [4] Gross, M.; Haroche, S. *Phys. Rep.* **1982**, *93*, 301–396.
- [5] Eberly, J.H. *J. Phys. B: At. Mol. Opt. Phys.* **2006**, *39*, S599–S604.
- [6] Scully, M.O.; Fry, E.S.; Ooi, C.H.R.; Wodkiewicz, K. *Phys. Rev. Lett.* **2006**, *96*, 010501.
- [7] Friedberg, R.; Manassah, J.T. *Laser Phys. Lett.* **2007**, *4*, 900–911.
- [8] Svidzinsky, A.A.; Chang, J.-T.; Scully, M.O. *Phys. Rev. Lett.* **2008**, *100*, 160504.
- [9] Scully, M.O.; Svidzinsky, A.A. *Phys. Rev. Lett.* **2009**, *373*, 1283–1286.
- [10] Scully, M.O. *Phys. Rev. Lett.* **2009**, *102*, 143601.
- [11] Prasad, S.; Glauber, R.J. *Phys. Rev. A* **2010**, *82*, 063805.
- [12] Svidzinsky, A.A.; Chang, J.-T.; Scully, M.O. *Phys. Rev. A* **2010**, *81*, 053821.
- [13] Friedberg, R.; Manassah, J.T. *Phys. Rev. A* **2010**, *81*, 063822.
- [14] Friedberg, R.; Manassah, J.T. *Phys. Lett. A* **2010**, *374*, 1648–1659.
- [15] Roehlsberger, R.; Schlage, K.; Sahoo, B.; Couet, S.; Ruffer, R. *Science* **2010**, *328*, 1239–1241.
- [16] Bienaimé, T.; Bux, S.; Lucioni, E.; Courteille, Ph.W.; Piovella, N.; Kaiser, R. *Phys. Rev. Lett.* **2010**, *104*, 183602.
- [17] Bender, H.; Stehle, C.; Slama, S.; Kaiser, R.; Piovella, N.; Zimmermann, C.; Courteille, Ph.W. *Phys. Rev. A* **2010**, *82*, 011404.
- [18] Courteille, Ph.W.; Bux, S.; Lucioni, E.; Lauber, K.; Bienaimé, T.; Kaiser, R.; Piovella, N. *Eur. J. Phys. D* **2010**, *58*, 69–73.
- [19] Kaiser, R. *J. Mod. Opt.* **2009**, *56*, 2082–2088.
- [20] Bux, S.; Lucioni, E.; Bender, H.; Bienaimé, T.; Lauber, K.; Stehle, C.; Zimmermann, C.; Slama, S.; Courteille, Ph.W.; Piovella, N.; Kaiser, R. *J. Mod. Opt.* **2010**, *57*, 1841–1848.
- [21] Greentree, A.; Tahan, C.; Cole, J.; Hollenberg, L. *Nat. Phys.* **2006**, *2*, 856–861.
- [22] Osterloh, A.; Amico, L.; Falci, G.; Fazio, R. *Nature* **2002**, *416*, 608–610.
- [23] Akkermans, E.; Gero, A.; Kaiser, R. *Phys. Rev. Lett.* **2008**, *101*, 103602.
- [24] Scully, M.O.; Zubairy, S. *Quantum Optics*; Cambridge University Press: Cambridge, 1997.
- [25] Agarwal, G.S. In *Quantum Statistical Theories of Spontaneous Emission and their Relation to other Approaches*: Höhler, G., Ed.; Springer Tract in Modern Physics; Springer-Verlag: Berlin, 1974.
- [26] van de Hulst, H.C. *Light Scattering by Small Particles*; Dover Publications: New York, 1981.
- [27] Dalibard, J. Le rôle des Fluctuations dans la Dynamique d'un Atome Couplé au Champ Électromagnétique. Ph.D.; Université Pierre et Marie Curie – Paris VI, 1986.
- [28] Gordon, J. *Phys. Rev. A* **1973**, *8*, 14–21.
- [29] Campbell, G.; Leonhardt, A.E.; Mun, J.; Boyd, M.; Streed, E.W.; Ketterlee, W. *Phys. Rev. Lett.* **2005**, *94*, 170403.
- [30] Sargent, M. III; Scully, M.O.; Lamb, W.E. *Laser Physics*; Addison-Wesley: Reading, MS, 1974; p 400.
- [31] Labeyrie, G., et al. *Phys. Rev. Lett.* **2003**, *91*, 223904.

Appendix 1. Evaluation of the integral kernel in Equation (6)

Let's consider the last term in Equation (6) and pass to the continuous frequency approximation:

$$I(\mathbf{r}_{jm}) = \sum_{\mathbf{k}} g_{\mathbf{k}}^2 \exp(i\mathbf{k} \cdot \mathbf{r}_{jm}) \int_0^t dt' \hat{\sigma}_m(t-t') \exp[-ic(k-k_0)t'] \\ \rightarrow \frac{V_{\text{ph}}}{(2\pi)^3} \int d\mathbf{k} g_{\mathbf{k}}^2 \exp(i\mathbf{k} \cdot \mathbf{r}_{jm}) \int_0^t dt' \hat{\sigma}_m(t-t') \exp[-ic(k-k_0)t'] \quad (52)$$

We exchange the integration order and introduce spherical coordinates, $d\mathbf{k} = dk k^2 d\phi d\theta \sin\theta$. After integration of the angular part, we obtain

$$I(\mathbf{r}_{jm}) = \frac{V_{\text{ph}}}{2\pi^2} \int_0^t dt' \hat{\sigma}_m(t-t') \exp(ick_0 t') \\ \times \int_0^\infty dk k^2 g_{\mathbf{k}}^2 \frac{\sin(kr_{jm})}{kr_{jm}} \exp(-ickt'), \quad (53)$$

where $r_{jm} = |\mathbf{r}_{jm}|$. We approximate the k integral as

$$\int_0^\infty dk k^2 g_{\mathbf{k}}^2 \frac{\sin(kr_{jm})}{kr_{jm}} \exp(-ickt') \\ \approx \frac{k_0^2 g_{k_0}^2}{2ik_0 r_{jm}} \int_{-\infty}^\infty dk \{ \exp[-ick(t' - r_{jm}/c)] - \exp[-ick(t' + r_{jm}/c)] \}, \quad (54)$$

where we made the following approximations: (a) we assumed the spectrum centered around $k \approx k_0$, so that $kg_{\mathbf{k}}^2 \approx k_0 g_{k_0}^2$; (b) we extended the lower integration value from 0 to $-\infty$, thus recovering the nonresonant term beyond the RWA. Using the expression above, we write

$$I(\mathbf{r}_{jm}) = \frac{\Gamma}{2ik_0 r_{jm}} \int_0^t dt' \hat{\sigma}_m(t-t') \exp(ick_0 t') \\ \times \{ \delta(t' - r_{jm}/c) - \delta(t' + r_{jm}/c) \} \\ = \frac{\Gamma}{2} \frac{\exp(ik_0 r_{jm})}{ik_0 r_{jm}} \hat{\sigma}_m(t - r_{jm}/c), \quad (55)$$

where $\Gamma = V_{\text{ph}} k_0^2 g_{k_0}^2 / (\pi c)$. We observe that this approach does not require one to assume the Markov approximation before solving the time integral, as in the standard approach [12]. On the contrary, this approach allows one to obtain the retarded (or non-local) kernel, which, when the 'rapid transit approximation' is assumed, i.e. $\hat{\sigma}_m(t - r_{jm}/c) \approx \hat{\sigma}_m(t)$, reduces to the exponential kernel of Equation (8).

Appendix 2. Collective Lamb shift for a Gaussian distribution

Let consider Equation (33) for a continuous distribution:

$$A_\infty = -\frac{\Gamma N}{8\pi^2} \mathbf{P} \int_0^\infty \frac{d\kappa \kappa^3}{\kappa - 1} \int_0^{2\pi} d\phi \int_0^\pi d\theta \sin\theta |S_\infty(\kappa, \theta, \phi)|^2. \quad (56)$$

A spherical Gaussian distribution, $n(r)_0 \exp(-r^2/2\sigma_R^2)$, yields $S_\infty(\kappa, \theta, \phi) = \exp[-\sigma^2(\kappa^2 + 1 - 2\kappa \cos\theta)/2]$, where $\sigma = k_0 \sigma_R$. Inserting it in Equation (56) we obtain

$$A_\infty = -\frac{\Gamma N}{4\pi} \mathbf{P} \int_0^\infty \frac{d\kappa \kappa^3}{\kappa - 1} \exp[-\sigma^2(\kappa^2 + 1)] \int_0^\pi d\theta \sin\theta \exp(2\sigma^2 \kappa \cos\theta) \\ = -\frac{\Gamma N}{8\pi\sigma^2} \mathbf{P} \int_0^\infty \frac{d\kappa \kappa^2}{\kappa - 1} [\exp[-\sigma^2(\kappa - 1)^2] - \exp[-\sigma^2(\kappa^2 + 1)^2]] \\ = -\frac{\Gamma N}{8\pi\sigma^2} \mathbf{P} \int_0^\infty d\kappa \left(\kappa + 1 + \frac{1}{\kappa - 1} \right) [\exp[-\sigma^2(\kappa - 1)^2] \\ - \exp[-\sigma^2(\kappa + 1)^2]] \\ = -\frac{\Gamma N}{8\pi\sigma^2} \mathbf{P} \int_{-1}^\infty dx \left(2 + x + \frac{1}{x} \right) [\exp(-\sigma^2 x^2) \\ - \exp[-\sigma^2(2+x)^2]]. \quad (57)$$

For $\sigma \gg 1$ it is approximated by

$$A_\infty \approx -\frac{\Gamma N}{8\pi\sigma^2} \mathbf{P} \int_{-1}^\infty dx \left(2 + \frac{1}{x} \right) \exp(-\sigma^2 x^2) \approx -\frac{\Gamma N}{4\pi^{1/2} \sigma^3}, \quad (58)$$

in agreement with the result of Friedberg and Manassah [14].